J. Math. Study
doi: 10.4208/jms.v48n4.15.03

Vol. **48**, No. 4, pp. 345-361
December 2015

Numerical Approximations of the Spectral Discretization of Flame Front Model

Jun Zhang[1], Wu-lan Li[2,*], Xin-Yue Fan[3], and Xiao-Jun Yu[4]

[1] *School of Mathematics and Statistical, Guizhou University of Finance and Econmics, Guiyang 550025, P. R. China.*
[2] *College of Information Science and Computer Engineering, Wenzhou Medical University, Wenzhou, Zhejiang 325035, P. R. China.*
[3] *College of Science Guizhou University, 550025 Guiyang, P. R. China.*
[4] *School of Mathematics and Statistical, Guizhou University of Finance and Econmics, Guiyang 550025, P. R. China.*

Received 13 April, 2015; Accepted 3 November, 2015

Abstract. In this paper, we consider the numerical solution of the flame front equation, which is one of the most fundamental equations for modeling combustion theory. A schema combining a finite difference approach in the time direction and a spectral method for the space discretization is proposed. We give a detailed analysis for the proposed schema by providing some stability and error estimates in a particular case. For the general case, although we are unable to provide a rigorous proof for the stability, some numerical experiments are carried out to verify the efficiency of the schema. Our numerical results show that the stable solution manifolds have a simple structure when β is small, while they become more complex as the bifurcation parameter β increases. At last numerical experiments were performed to support the claim the solution of flame front equation preserves the same structure as K-S equation.

AMS subject classifications: 65N35, 65T50, 65L12, 65M70.

Key words: Flame front equation, Finite difference, Fourier method, Error estimates.

1 Introduction

The reduction of a free-interface problem to an explicit equation for the interface dynamics is a challenging issue and much research on this subject has been carried out during decade. A paradigm of two-dimensional problem in combustion theory is the model for the Near Equidiffusive Flames (NEF), which was introduced by Matkowsky

*Corresponding author. *Email addresses:* zj654440@email (J. Zhang), liwulan@163.com (W. L. Li), fan.xinyue@163.com (X. Y. Fan), xjyu-myu@163.com (X. J. Yu)

and Sivashinsky [17] in 1979, this equation is characterized by near-unity Lewis numbers, near-adiabatic flame temperatures and near-uniform enthalpies. For the moving flame front, defined by $x=\xi(t,y)$, the temperature θ and enthalpy S, one ends up with the free-interface problem:

$$\frac{\partial\theta}{\partial t}=\Delta\theta,\ x<\xi(t,y), \tag{1.1}$$

$$\theta=1,\ x\geq\xi(t,y), \tag{1.2}$$

$$\frac{\partial S}{\partial t}=S-\alpha\Delta\theta,\ x\neq\xi(t,y). \tag{1.3}$$

At the front, θ and S are continuous and the following jump conditions occur for the normal derivatives:

$$\left[\frac{\partial\theta}{\partial n}\right]=-\exp(S),\qquad \left[\frac{\partial S}{\partial n}\right]=\alpha\left[\frac{\partial\theta}{\partial n}\right], \tag{1.4}$$

where α is the reduced Lewis number. This equation provides a convenient framework for the theoretical study of a number of flame phenomena. Sivashinsky [21] considered the constant-density model of a premixed flame, and he derived an asymptotic Kuramoto-Sivashinsky (K-S) equation, which describes the evolution of the disturbed flame front:

$$\partial_\tau\Phi+4\partial_\eta^4\Phi+\partial_\eta^2\Phi+\frac{1}{2}(\partial_\eta\Phi)^2=0.$$

Brauner and Lunardi [7] proved instability of the planar travelling wave solution in a two-dimensional free boundary problem stemmed by the propagation of premixed flames. Lorenzi [16] dealt with a free boundary problem, modelling the propagation of premixed flames in a infinite strip in $\mathbb{R}^2$, he proved existence, uniqueness, regularity results for the solutions near the travelling wave. Ducrot and Marion [11] considered a semi-linear elliptic system in combustion theory. In particular, they proved the existence of travelling wave solutions for high activation energy. Brauner *et al.* [5] obtained a simplified quasisteady version of NEF, this simplifiecation allows near the planar front, an explicit derivation of the front equation. And they introduced a parameter ε, rescale both the dependent and independent variables, and proved rigourously the convergence to the solution of the K-S equation as $\varepsilon\to 0$. In [2], Berestycki *et al.* presented a Burgers-Sivashinsky (B-S) equation, a model pertinent to the flame front dynamics subject to the buoyancy effect. Later, Brauner *et al.* [4] derived a quasi-steady (Q-S) equation, a quasi-steady version of the κ-θ in flame theory. Both of two dissipative systems have similar dynamics. A previous work [6] by Brauner *et al.* were concerned with a generalized K-S equation, which is a nonlinear wave equation with a strong damping operator. There are alternative possibilities for reduction of the free-interface problem (1.1)-(1.4) to an explicit equation of the flame front. In other words, starting from the same configuration,

the solution of following equation:

$$4\varepsilon^2\partial_t^2 u+\partial_t u-8\varepsilon\partial_x^2\partial_t u+4\partial_x^4 u+\beta(\partial_x^2 u+\frac{1}{2}(\partial_x u)^2-\frac{1}{4\pi}\int_0^{2\pi}(\partial_x u(\cdot,t))^2 ds)=0, \tag{1.5}$$

$$u(x,t)=u(x+2\pi,t),u(x,0)=u_0(x),\ \partial_t u(x,0)=u_1(x) \tag{1.6}$$

remains on a fixed time interval close to the solution of K-S equation for moderately small values of ε.

Some other work have been focused on using numerical methods to simulate the behavior of the free-interface problem. The pioneering work is due to Hyman and Nicloenko ([12], [13]), in accordance with Turing's prediction (see [22]) K-S equation generates a cellular structure, pattern formation, and chaotic behavior in appropriate range of parameters. For a large review of methods for investigating the solutions of K-S equation, we refer to ([1], [10], [14], [15]) and its extensive bibliography.

In this paper, we will propose a finite difference/spectral schema for the flame front equation (1.5)-(1.6). The proposed schemes combine a second order finite difference approach in time and Fourier spectral method in space. For bifurcation parameter β=0, stability analysis and error estimates are carried out for the linear flame front equation. As β/=0, a series of numerical examples are presented to confirm the efficiency of the schema. The purpose of the numerical experiments are presented to investigate the behavior of the solution of flame front equation as compared to the K-S equation for moderately small values of ε. Our numerical experiments show that the stable solution manifolds have a simple structure when β is small. As the bifurcation parameter β increase, the stable solution manifolds become more complex. Finally several numerical examples are provided to support the well-known claim that the flame front equation asymptotically converges to the K-S equation, and its solution preserves the same structure as the K-S equation.

The paper is organized as follows. In section 2, a schema combining a second order finite difference approach in the time direction and a spectral method in the space is reviewed and it's stability and convergence are analyzed. In section 3, numerical experiments are presented to investigate the behavior of the solution of flame front equation. Finally, some concluding remarks are drawn in section 4.

2 Flame front equation and discretisation in time

As $\beta=0$, we first consider the linear flame front equation as follows:

$$4\varepsilon^2\partial_t^2 u+\partial_t u-8\varepsilon\partial_x^2\partial_t u+4\partial_x^4 u=0,\ (x,t)\in(0,2\pi)\times(0,T], \tag{2.1}$$

$$u(x,t)=u(x+2\pi,t),\ (x,t)\in[0,2\pi]\times(0,T], \tag{2.2}$$

$$u(x,0)=u_0(x),\ \partial_t u(x,0)=u_1(x),\ x\in[0,2\pi]. \tag{2.3}$$

We consider in this section the numerical analysis of a commonly used schema for the flame front equation (2.1)-(2.3) in the case of periodic boundary condition in the bounded domain $\Lambda := (0,2\pi)$. To this end, we need some functional spaces that will be used hereafter to define the variational formulation. We use $H^m(\Lambda)$ and $\|\cdot\|_m (m=0,\pm1,\dots)$ to denote the standard Sobolev spaces and their norms, respectively. In particular, the norm and inner product of $L^2(\Lambda)=H^0(\Lambda)$ are denoted by $\|\cdot\|_0$, and $(\cdot,\cdot)$ respectively.

2.1 Stability analysis

In order to study stability property, we will use a discrete energy estimate. To this end, we first state the following result.

Lemma 2.1. *The solution u of the problem* (2.1)-(2.3) *satisfies the following energy inequality:*

$$E(u)\leq E(u_0),$$

where

$$E(u)=2\varepsilon^2\|\partial_t u\|_0^2+2\|\partial_x^2 u\|_0^2.$$

Proof. Computing the inner product of (2.1) with $\partial_t u$, then we have

$$2\varepsilon^2\frac{d}{dt}\|\partial_t u\|_0^2+\|\partial_t u\|_0^2+8\varepsilon\|\partial_x\partial_t u\|_0^2+2\frac{d}{dt}\|\partial_x^2 u\|_0^2=0.$$

This results in

$$\frac{d}{dt}E(u)\leq 0.$$

The lemma is proved. □

Second-order schema in time. First, we introduce a second order finite difference schema to discretize the time. For a given integer $K\geq 0$, let $t_n=n\Delta t, n=0,1,\dots,K$, where $\Delta t=T/K$ is the time step.

Then we propose the following finite difference schema for the time discretization of (2.1)-(2.3):

$$4\varepsilon^2\frac{u^{n+1}-2u^n+u^{n-1}}{\Delta t^2}+\frac{u^{n+1}-u^{n-1}}{2\Delta t}-8\varepsilon\frac{\partial_x^2u^{n+1}-\partial_x^2u^{n-1}}{2\Delta t}+2(\partial_x^4u^{n+1}+\partial_x^4u^{n-1})=0, n\geq 1. \tag{2.4}$$

The stability result for the schema (2.4) is given in the following lemma.

Lemma 2.2. *The time-discretized problem* (2.4) *is unconditionally stably in the sense that* $\forall\ \Delta t \geq 0$, *the following energy inequality holds:*

$$E(u^n) \leq E(u^{n-1}),\ \ n \geq 1,$$

where

$$E(u^n) = 4\varepsilon^2 \left\| \frac{u^{n+1}-u^n}{\Delta t} \right\|_0^2 + 2(\|\partial_x^2 u^{n+1}\|_0^2 + \|\partial_x^2 u^n\|_0^2).$$

Proof. For all φ, it follows from (2.4) that

$$\begin{aligned}\frac{4\varepsilon^2}{\Delta t^2}(u^{n+1}-2u^n+u^{n-1},\varphi) + \frac{1}{2\Delta t}(u^{n+1}-u^{n-1},\varphi) + \frac{4\varepsilon}{\Delta t}(\partial_x u^{n+1}-\partial_x u^{n-1},\partial_x\varphi)\\ +2(\partial_x^2 u^{n+1}+\partial_x^2 u^{n-1},\partial_x^2\varphi)=0,\ \ n\geq 1.\end{aligned}$$

Letting $\varphi = u^{n+1}-u^{n-1}$ gives

$$\begin{aligned}&\frac{4\varepsilon^2}{\Delta t^2}(\|u^{n+1}-u^n\|_0^2 - \|u^n-u^{n-1}\|_0^2) + \frac{1}{2\Delta t}\|u^{n+1}-u^{n-1}\|_0^2\\ &+\frac{4\varepsilon}{\Delta t}\|\partial_x u^{n+1}-\partial_x u^{n-1}\|_0^2 + 2\|\partial_x^2 u^{n+1}\|_0^2 - 2\|\partial_x^2 u^{n-1}\|_0^2 = 0,\ \ n\geq 1.\end{aligned}$$

The proof is completed. □

2.2 Error analysis

Since the underlying problem is subject to the periodic boundary condition, the Fourier method is undoubtedly among the first ones to provide efficient solutions (see [3], [9], [23], [24]). In this section, we consider a Fourier spectral approximation in space for the semi-discrete problems presented in the previous section.

We first introduce some notations and basic approximation results for the spectral approximation. Let

$$S_N = \text{span}\{\exp(-\imath kx),\ -N \leq k \leq N\},$$

we denote by π_N the usual L^2-projection operator, i.e., for all $v \in L^2(\Lambda)$, $\pi_N v \in S_N$, such that

$$(\pi_N v - v, \psi) = 0, \qquad \forall \psi \in S_N.$$

Similarly we define the H^2-projection operator $\pi_N^1 : H_*^2(\Lambda) \to S_N$ by

$$(\partial_x^2(\pi_N^1 v - v), \partial_x^2 \psi) = 0, \qquad \forall \psi \in S_N,$$

where $H^2_*(\Lambda)=\{v\in L^2(\Lambda),\partial^k_x v\in L^2(\Lambda),\text{for all positive integer } k\leq 2\}$. We know the following estimates hold [8], [20]:

$$\|v-\pi_N v\|_0\leq cN^{-m}\|v\|_m,\qquad \forall v\in H^m_*(\Lambda),m\geq 0; \tag{2.5}$$

$$\|v-\pi^1_N v\|_k\leq cN^{k-m}\|v\|_m,\ k=0,1,2;\qquad \forall v\in H^m_*(\Lambda),m\geq 2. \tag{2.6}$$

Second-order schema in time/spectral method in space. The spatial discretisation to the semi-discrete problem (2.4) consists in finding an approximate solution $u^{n+1}_N(x)$ in form of a truncated Fourier expansion:

$$u^{n+1}_N(x)=\sum_{k=-N/2}^{N/2-1}\hat{u}^{n+1}_k\exp(-\imath kx),$$

which satisfies the following weak formulation with $u^0_N=\pi_N u_0$, $n\geq 1$:

$$\begin{aligned}\frac{4\varepsilon^2}{\Delta t^2}(u^{n+1}_N-2u^n_N+u^{n-1}_N,\varphi_N)+\frac{1}{2\Delta t}(u^{n+1}_N-u^{n-1}_N,\varphi_N)+\frac{4\varepsilon}{\Delta t}(\partial_x u^{n+1}_N-\partial_x u^{n-1}_N,\partial_x\varphi_N)\\ +2(\partial^2_x u^{n+1}_N+\partial^2_x u^{n-1}_N,\partial^2_x\varphi_N)=0,\qquad \forall\varphi_N\in S_N.\end{aligned} \tag{2.7}$$

For the full discrete problem (2.7), following exactly the same lines as in lemma 2.2, we can derive some similar energy inequality, which is stated in the following lemma without a detailed proof.

Lemma 2.3. *The solution of the full discrete problem* (2.7) *satisfies*

$$E(u^n_N)\leq E(u^{n-1}_N),\ n=1,2,\ldots,K-1.$$

Next we carry out an error analysis for the full discrete problems (2.7). First, let us denote

$$\tilde{e}^n=\pi^1_N u(\cdot,t_n)-u^n_N,\ \ \hat{e}^n=u(\cdot,t_n)-\pi^1_N u(\cdot,t_n),\ \ e^n=u(\cdot,t_n)-u^n_N=\tilde{e}^n+\hat{e}^n,$$

and the truncation error $R^n=4\varepsilon^2R^n_1+R^n_2+4R^n_3+8\varepsilon R^n_4, n\geq 0$, where

$$\begin{aligned}R^n_1(x)&:=\frac{u(x,t_{n+1})-2u(x,t_{n+1})+u(t_{n-1})}{\Delta t^2}-\partial^2_t u(x,t_n),\\ R^n_2(x)&:=\frac{u(x,t_{n+1})-u(x,t_{n-1})}{2\Delta t}-\partial_t u(x,t_n),\\ R^n_3(x)&:=\frac{\partial^4_x u(x,t_{n+1})+\partial^4_x u(x,t_{n-1})}{2}-\partial^4_x u(x,t_n),\\ R^n_4(x)&:=\partial^2_x\partial_t u(x,t_n)-\frac{\partial^2_x u(x,t_{n+1})-\partial^2_x u(x,t_{n-1})}{2\Delta t}.\end{aligned}$$

A direct calculation using the Taylor series gives immediately the following estimates:

$$\|R\|_0\leq c\Delta t^2. \tag{2.8}$$

We start by deriving an error estimate for the full discrete problem (2.7) in the next theorem.

Theorem 2.1. *Let u be the exact solution of* (2.1), *$\{u_N^n\}_{n=0}^M$ be the discrete solution of* (2.7). *If u is smooth enough (at least second order differentiable in t, m-order differentiable in x), then the following error estimate holds:*

$$\varepsilon\Big\|\frac{u(\cdot,t_{k+1})-u(\cdot,t_k)}{\Delta t}-\frac{u_N^{k+1}-u_N^k}{\Delta t}\Big\|_0+\|\partial_x^2u(\cdot,t_k)-\partial_x^2u_N^k\|_0\le c(\Delta t^2+N^{2-m}),\ k\ge0, \quad (2.9)$$

where c dependent on T,u, and $1/\varepsilon$.

Proof. Subtracting (2.7) from a reformulation of (2.1) at t_{n+1}, we obtain

$$\begin{aligned}
&\frac{4\varepsilon^2}{\Delta t^2}\big(\tilde e^{n+1}-2\tilde e^n+\tilde e^{n-1},\varphi_N\big)+\frac{1}{2\Delta t}\big(\tilde e^{n+1}-\tilde e^{n-1},\varphi_N\big)\\
&+2\big(\partial_x^2(\tilde e^{n+1}+\tilde e^{n-1}),\partial_x^2\varphi_N\big)+\frac{4\varepsilon}{\Delta t}\big(\partial_x(\tilde e^{n+1}-\tilde e^{n-1}),\partial_x\varphi_N\big)\\
=&(R^n,\varphi_N)+\frac{4\varepsilon^2}{\Delta t^2}\Big(\big(\pi_N^1-I\big)\big(u(\cdot,t_{n+1})-2u(\cdot,t_n)+u(\cdot,t_{n-1})\big),\varphi_N\Big)\\
&+\frac{1}{2\Delta t}\Big(\big(\pi_N^1-I\big)\big(u(\cdot,t_{n+1})-u(\cdot,t_{n-1})\big),\varphi_N\Big)\\
&-\frac{4\varepsilon}{\Delta t}\Big(\big(\pi_N^1-I\big)\big(\partial_x^2(u(\cdot,t_{n+1})-u(\cdot,t_{n-1}))\big),\varphi_N\Big).
\end{aligned}\quad (2.10)$$

Taking $\varphi_N=\tilde e^{n+1}-\tilde e^{n-1}$, we arrive at

$$\begin{aligned}
E(\tilde e^n)-E(\tilde e^{n-1})\le&\frac{\Delta t}{2\varepsilon^2}\|R^n\|_0^2+\varepsilon^2\Delta t\Big(\Big\|\frac{\tilde e^{n+1}-\tilde e^n}{\Delta t}\Big\|_0^2+\Big\|\frac{\tilde e^n-\tilde e^{n-1}}{\Delta t}\Big\|_0^2\Big)\\
&+4\varepsilon^2\Big[2\Delta t\|(\pi_N^1-I)\partial_t^2u(\cdot,t)\|_0^2+\frac{\Delta t}{4}\Big(\Big\|\frac{\tilde e^{n+1}-\tilde e^n}{\Delta t}\Big\|_0^2+\Big\|\frac{\tilde e^n-\tilde e^{n-1}}{\Delta t}\Big\|_0^2\Big)\Big]\\
&+\frac{\Delta t}{2\varepsilon^2}\|(\pi_N^1-I)\partial_tu(\cdot,t)\|_0^2+\varepsilon^2\Delta t\Big(\Big\|\frac{\tilde e^{n+1}-\tilde e^n}{\Delta t}\Big\|_0^2+\Big\|\frac{\tilde e^n-\tilde e^{n-1}}{\Delta t}\Big\|_0^2\Big)\\
&+8\varepsilon\Big[\frac{4\Delta t}{\varepsilon}\|(\pi_N^1-I)\partial_x^2\partial_tu(\cdot,t)\|_0^2+\frac{\varepsilon\Delta t}{8}\Big(\Big\|\frac{\tilde e^{n+1}-\tilde e^n}{\Delta t}\Big\|_0^2+\Big\|\frac{\tilde e^n-\tilde e^{n-1}}{\Delta t}\Big\|_0^2\Big)\Big].
\end{aligned}$$

Summing up the above inequality for $n=1,2,\dots,k$, dropping some unnecessary terms and observing (2.8), we find

$$E(\tilde e^k)-E(\tilde e^0)\le\Delta t\sum_{n=1}^k\Big(E(\tilde e^n)+E(\tilde e^{n-1})\Big)+c\Big(\frac{\Delta t^4}{\varepsilon^2}+\frac{1}{\varepsilon^2}N^{-2m}+N^{4-2m}\Big),\ k\ge1. \quad (2.11)$$

Finally, the desired result (2.9) follows from the discrete Gronwall lemma to (2.10) and the triangular inequality. □

3 Numerical experiments

3.1 The numerical schema

We describe in this section the numerical schema to approximate solutions of (1.5)-(1.6). A complete numerical algorithm requires a discreteization strategy in both time and space. Since the Fourier method is one of the most suitable approximation for periodic problems, it will be employed to handle the spatial discretization. The time discretization combines a Newmark schema for the second-order derivative in time, Crank-Nicolson schema for the first-order derivative in time, implicit treatment for all linear terms and explicit treatment for all nonlinear terms. Precisely, the time schema reads:

$$\begin{aligned}&\frac{4\varepsilon^2}{\Delta t^2}(u^{n+1}-2u^n+u^{n-1})-\frac{4\varepsilon}{\Delta t}(\partial_x^2u^{n+1}-\partial_x^2u^{n-1})+\frac{1}{2\Delta t}(u^{n+1}-u^{n-1})\\&+2(\partial_x^4u^{n+1}+\partial_x^4u^{n-1})+\frac{\beta}{2}(\partial_x^2u^{n+1}+\partial_x^2u^{n-1})=\frac{\beta}{4\pi}\int_0^{2\pi}(\partial_xu^n)^2dx-\frac{\beta}{2}(\partial_xu^n)^2,\end{aligned}\tag{3.1}$$

for $n\geq 1$,

$$\begin{aligned}&\frac{4\varepsilon^2}{\Delta t^2}(2u^1-2u^0-2\Delta tu_1)+u_1-8\varepsilon\partial_x^2u_1+2(2\partial_x^4u^1-2\Delta t\partial_x^4u_1)\\&+\frac{\beta}{2}(2\partial_x^2u^1-2\Delta t\partial_x^2u_1)=\frac{\beta}{4\pi}\int_0^{2\pi}(\partial_xu^0)^2dx-\frac{\beta}{2}(\partial_xu^0)^2,\end{aligned}\tag{3.2}$$

for the first step calculation. The initial conditions are given by

$$u(x,0)=u_0(x),\ \partial_tu(x,0)=u_1(x)=-\left(4\partial_x^4u_0(x)+\partial_x^2u_0(x)+\frac{1}{2}(\partial_xu_0(x))^2\right).\tag{3.3}$$

This method is of second order accuracy with respect to the time step. The use of such a schema is motivated by the following consideration: the implicit treatment of the fourth and second-order terms allows to reduce the associated stability constraint nonlinear terms avoids the expensive process of solving nonlinear equation at each time step.

We start with some implementation details. By applying the Fourier transformation to (3.1), we obtain a linear system for the Fourier modes $\{\hat{u}_k^{n+1}\}_{k=-N/2}^{N/2-1}$:

$$\begin{aligned}&\frac{4\varepsilon^2}{\Delta t^2}(\hat{u}_k^{n+1}-2\hat{u}_k^n+\hat{u}_k^{n-1})+\frac{4\varepsilon k^2}{\Delta t}(\hat{u}_k^{n+1}-\hat{u}_k^{n-1})+\frac{1}{2\Delta t}(\hat{u}_k^{n+1}-\hat{u}_k^{n-1})\\&+2k^4(\hat{u}_k^{n+1}+\hat{u}_k^{n-1})-\frac{k^2\beta}{2}(\hat{u}_k^{n+1}+\hat{u}_k^{n-1})=\left\{\frac{\beta}{4\pi}\int_0^{2\pi}(\partial_xu^n)^2dx-\frac{\beta}{2}(\partial_xu^n)^2\right\}_k,\end{aligned}\tag{3.4}$$

where, $\hat{f}_k$, or $\{f\}_k$ also represents the kth Fourier coefficient of the function f. The Fourier coefficients of the nonlinear terms are calculated by performing the discrete fast Fourier transform (FFT). In practical calculations, we work in the spectral space. An additional

FFT is needed to recover the physical nodal values $u_k(-K\leq k\leq K)$ from $\hat{u}$. By using (3.4) the kth Fourier coefficient $\hat{u}_k^{n+1}$ can be obtained by a simple inversion

$$\hat{u}_k^{n+1}=\left[\frac{4\varepsilon^2}{\Delta t^2}+\frac{1}{2\Delta t}+\left(\frac{4\varepsilon k}{\Delta t}-\frac{\beta}{2}\right)k^2+2k^4\right]^{-1}\left[\frac{8\varepsilon^2}{\Delta t^2}\hat{u}_k^n\right.$$
$$\left.+\left(-\frac{4\varepsilon^2}{\Delta t^2}+\frac{1}{2\Delta t}+\left(\frac{4\varepsilon k}{\Delta t}+\frac{\beta}{2}\right)k^2-2k^4\right)\hat{u}_k^{n-1}+\left\{\frac{\beta}{4\pi}\int_0^{2\pi}(\partial_x u^n)^2dx-\frac{\beta}{2}(\partial_x u^n)^2\right\}_k\right]. \tag{3.5}$$

For the first step, it is

$$\hat{u}_k^1=\left[\frac{8\varepsilon^2}{\Delta t^2}+4k^4-\beta k^2\right]^{-1}\left\{\frac{8\varepsilon^2}{\Delta t^2}(u_0+\Delta t u_1)-u_1+8\varepsilon\partial_x^2u_1\right.$$
$$\left.+4\Delta t\partial_x^4u_1+\beta\Delta t\partial_x^2u_1+\left(\frac{\beta}{4\pi}\int_0^{2\pi}(\partial_x u_0)^2dx-\frac{\beta}{2}(\partial_x u_0)^2\right)\right\}_k. \tag{3.6}$$

3.2 Verification of the convergence order

The convergence rate is measured through computing the quantity:

$$p_1=\log_2\left(\frac{\|u_N^{n,2\Delta t}-u_N^{2n,\Delta t}\|_0}{\|u_N^{2n,\Delta t}-u_N^{4n,\Delta t/2}\|_0}\right),\quad p_2=\log_2\left(\frac{\|\partial_x^2u_N^{n,2\Delta t}-\partial_x^2u_N^{2n,\Delta t}\|_0}{\|\partial_x^2u_N^{2n,\Delta t}-\partial_x^2u_N^{4n,\Delta t/2}\|_0}\right), \tag{3.7}$$

where $u_N^{\cdot,\Delta t}$ means the solution obtained with the time step size Δt and Fourier mode number N. When initial datum $u_0(x)=\sin(x)$,$N=64$ and time $T=1$ are fixed, Tables 1-4 present the temporal convergence rate of discrete problem (3.4) for different β,ε and Δt. In Table 1, we list the computed rates for the schema (3.4) with $\beta=0$ for several time step sizes and ε. From this table, it is observed that the convergence rate is close to 2. This is in a good agreement with the result given in Theorem 2.1, which states that the convergence in time is of second order. In Tables 2-4, we list the convergence rates for the schema (3.5)-(3.6) with different parameters β. It is observed that the convergence rate is approach to second order, even though we can not get a priori error estimate for the convergence rate of the method, the numerical schema is still valid.

3.3 Convergence to K-S equation

This subsection is devoted to numerically investigate the behavior of the solution of equation (1.5)-(1.6) as compared to the K-S equation when $\varepsilon\to 0$. We first fix $\beta=10$, and let ε vary. In Figs. 1-3, we plot consecutive front positions with $u_0(x)=0.1(\sin(x)+\cos(x))$, for $\varepsilon=0.1$,$\varepsilon=0.01$, and $\varepsilon=0$ respectively. Note that the case $\varepsilon=0$ corresponds to the K-S

Table 1: Convergence rate in time with $\beta=0$ for different ε and Δt.

	$\varepsilon\backslash\Delta t$	Δt=1.00E-3	Δt=5.00E-4	Δt=2.00e-4	Δt=1.00E-4
p_1	$\varepsilon=0.1$	2.0000	2.0000	1.9990	1.9496
	$\varepsilon=0.05$	2.0000	2.0000	2.0002	2.0018
	$\varepsilon=0.02$	2.0000	2.0000	2.0000	2.0001
	$\varepsilon=0.01$	1.9999	2.0000	2.0000	2.0000
p_2	$\varepsilon=0.1$	1.9991	1.9998	2.0041	1.7883
	$\varepsilon=0.05$	2.0010	2.0003	1.9991	2.0077
	$\varepsilon=0.02$	1.9943	1.9986	1.9996	2.0004
	$\varepsilon=0.01$	1.9742	1.9935	1.9989	1.9998

Table 2: Convergence rate in time with $\beta=1$ for different ε and Δt.

	$\varepsilon\backslash\Delta t$	Δt=1.00E-3	Δt=5.00E-4	Δt=2.00e-4	Δt=1.00E-4
p_1	$\varepsilon=0.1$	1.9998	2.0001	2.0008	1.9950
	$\varepsilon=0.05$	1.9999	2.0000	1.9997	2.0029
	$\varepsilon=0.02$	1.9999	2.0000	2.0000	2.0001
	$\varepsilon=0.01$	2.0000	2.0000	2.0000	2.0000
p_2	$\varepsilon=0.1$	1.9997	2.0001	2.0046	1.9792
	$\varepsilon=0.5$	1.9988	1.9997	2.0002	2.0093
	$\varepsilon=0.02$	1.9935	1.9984	1.9998	1.9995
	$\varepsilon=0.01$	1.9765	1.9940	1.9991	1.9995

Table 3: Convergence rate in time with $\beta=4$ for different ε and Δt.

	$\varepsilon\backslash\Delta t$	Δt=1.00E-3	Δt=5.00E-4	Δt=2.00e-4	Δt=1.00E-4
p_1	$\varepsilon=0.1$	2.0000	2.0000	1.9999	2.0015
	$\varepsilon=0.05$	2.0001	2.0000	2.0000	2.0010
	$\varepsilon=0.02$	2.0009	2.0003	2.0000	2.0000
	$\varepsilon=0.01$	2.0029	2.0010	2.0002	2.0000
p_2	$\varepsilon=0.1$	2.0000	2.0000	1.9999	2.0022
	$\varepsilon=0.05$	2.0001	2.0000	2.0000	2.0010
	$\varepsilon=0.02$	2.0010	2.0003	2.0000	2.0000
	$\varepsilon=0.01$	2.0030	2.0011	2.0002	20000

equation. It is observed that the (x,t) contour plot of the solution close to the structure of K-S equation when ε tends to zero.

In order to quantify the convergence of the numerical solution for flame front equation as ε tends to zero, we compute the error $\|u_N^\varepsilon - u_N^{K-S}\|_{L^2}$, where u_N^ε is the solution of schema (3.4), u_N^{K-S} is the solution of schema (3.4) with $\varepsilon=0$. The discrete problems (3.4) is solved in the interval $(0,2\pi)$ with $\beta=10, N=64$, and $u_0=0.1(\sin(x)+\cos(x))$. All the numerical results reported in the Tables below have been evaluated at $T=10$.

Table 4: Convergence rate in time with $\beta=10$ for different ε and Δt.

	$\varepsilon\backslash\Delta t$	Δt=1.00E-3	Δt=5.00E-4	Δt=2.00e-4	Δt=1.00E-4
p_1	$\varepsilon=0.1$	1.9994	1.9999	1.9994	2.0008
	$\varepsilon=0.05$	2.0001	2.0000	1.9988	2.0084
	$\varepsilon=0.02$	2.0000	2.0000	2.0002	1.9995
	$\varepsilon=0.01$	2.0000	2.0000	2.0000	2.0002
p_2	$\varepsilon=0.1$	1.9999	2.0000	2.0002	1.9980
	$\varepsilon=0.05$	2.0011	2.0003	1.9998	2.0041
	$\varepsilon=0.02$	2.0009	2.0004	2.0003	1.9966
	$\varepsilon=0.01$	1.9896	1.9988	2.0014	1.9914

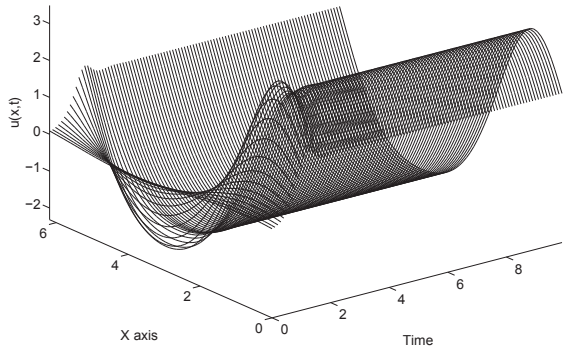

Figure 1: Flame front contour generated by (3.4) for $\varepsilon=0.1$.

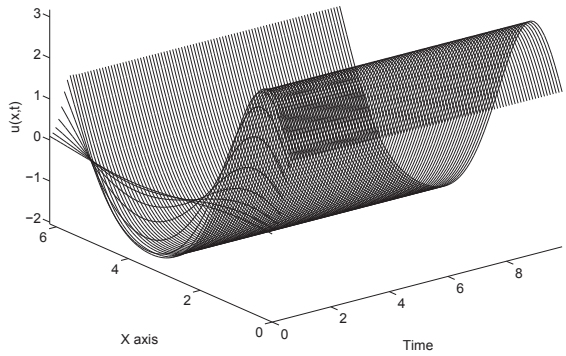

Figure 2: Flame front contour generated by (3.4) for $\varepsilon=0.01$.

In Table 5, we list the errors for the schema (3.4) with the different parameters. From this table, it is observed that schema (3.4) is of second-order accuracy in time as $\Delta t \ll \varepsilon$, and the error of the solution increases when ε becomes smaller. When $\varepsilon \to 0$, we can choose a sufficiently small Δt (at least $\Delta t = O(\varepsilon)$) such that the solution of schema (3.4) converge to the solution of the K-S equation.

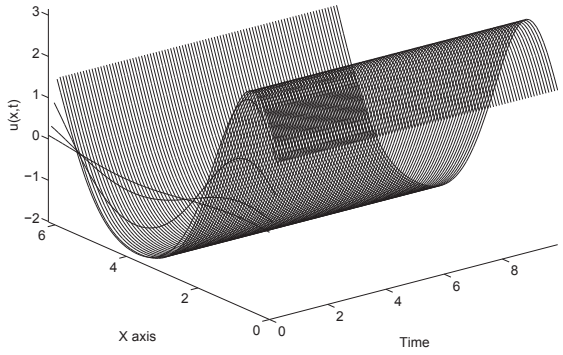

Figure 3: Flame front contour generated by (3.4) for $\varepsilon=0$.

Table 5: Errors for different ε and Δt.

	$\varepsilon\backslash\Delta t$	Δt=1.00E-2	Δt=5.00E-3	Δt=2.00E-3	Δt=1.00E-3
error	$\varepsilon=0.01$	7.78E-004	1.91E-004	2.63E-005	2.82E-006
	$\varepsilon=0.005$	-	7.82E-004	1.24E-004	3.01E-005
	$\varepsilon=0.002$	-	-	7.83E-004	1.96E-004
	$\varepsilon=0.001$	-	-	-	7.83E-004

Table 6: Errors for different ε and Δt.

	$\beta\backslash\Delta t$	Δt=1.00E-2	Δt=5.00E-3	Δt=2.00E-3	Δt=1.00E-3
error	$\beta=8$	7.78E-004	1.91E-004	2.63E-005	2.82E-006
	$\beta=10$	7.78E-004	1.91E-004	2.63E-005	2.82E-006
	$\beta=12$	-	1.91E-004	2.63E-005	2.82E-006

The influence of the parameter β on the error is presented in Table 6, where errors are listed for several β and Δt. Obviously, the impact of β on the error is not significant in Δt suitable small.

Remark 3.1. Brauner *et al.* [6] proved that the flame front equation asymptotic convergence to K-S equation as $\varepsilon\to 0$, numerical results show that we can choose $\Delta t=O(\varepsilon)$ such that the solution converge to the solution of K-S equation.

Nicolaeko *et al.* ([18], [19]) analyzed the stability of the solution by investigating the global dynamical properties of K-S. For periodic solutions, and they proved the constructive estate in the L^2-norm

$$\lim_{t\to\infty}\sup\left\|\frac{\partial u}{\partial x}(t)\right\|\leq \text{Const}\nu^{-1/4}\tilde{L}^{5/2}. \tag{3.8}$$

In order to investigate the dynamics of equation (1.5)-(1.6) with respect to the parameter β, in the discussion below, the energy is the integral of $(\partial_x u)^2$. In Fig. 4, we plot consecutive front positions and energy computed by (3.4)-(3.5) with β=2, $u_0=\sin(x)+\cos(x)$, $\varepsilon=$

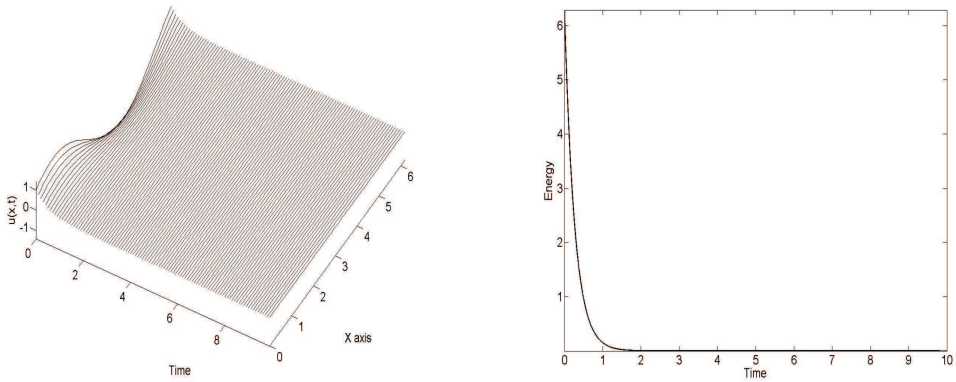

Figure 4: $\beta=2,\varepsilon=0.01,\Delta t=10^{-3}$, the contour of solution (left) and energy (right).

0.01, we observed that the solution and the energy decay almost to zero. We have confirmed that, similar the K-S equation, for $0\leq\beta\leq 4$, 0 is a global attractor for the solution to equation (1.5)-(1.6).

A non-trivial attractor is expected for a large β, the selected case is for $\beta=12$, $u_0=\sin x+\cos x$. Fig. 5 confirms that the solution gets attracted to a unimodal fixed point.

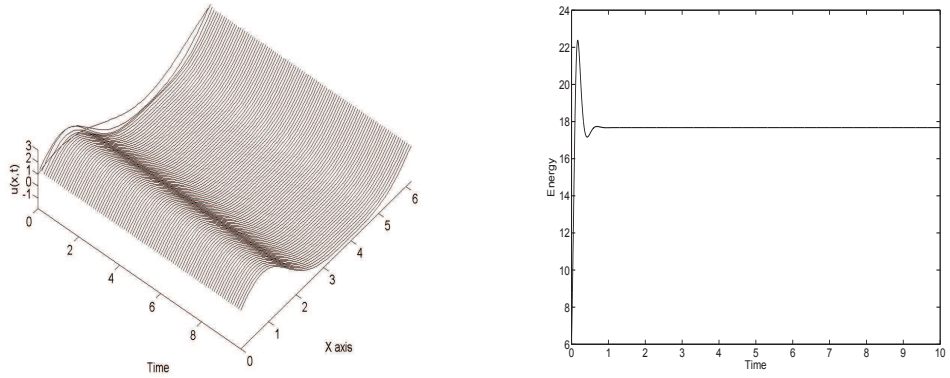

Figure 5: $\beta=12$, $\varepsilon=0.01$, $\Delta t=10^{-3}$ the contour of solution (left) and energy (right).

In Fig. 6, the front evolutions were generated by (3.4)-(3.5) with $\beta=17.3$, $u_0=\sin x+\cos x$, $\varepsilon=0.01$. We can see that the periodic orbits is clearly observed, the invariant circle remains globally attracting, and the (x,t) contour plot of the solution showes a phase shift at the bursts. Recall that the physical interpretation of the periodic problem is the dynamics on a cylindrical sample.

In Fig. 7, we plot the solution for $\beta=30$, $u_0=\sin x+\cos x$, $\varepsilon=0.001$. We observe that the solution lock into the pseudo-attracting bimodal fixed point, and the energy is nearly constant. When we take $\beta=60$, $u_0(x)=\cos(4x)$, $\varepsilon=0.001$, Fig. 8 exhibits that the front evolves lock onto an essentially trimodal orbit.

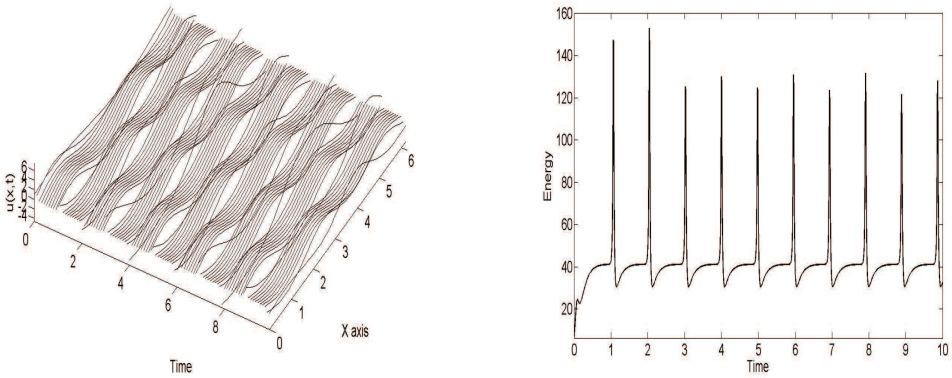

Figure 6: $\beta=17.3,\varepsilon=0.01,\Delta t=10^{-3}$, the contour of solution (left) and energy (right).

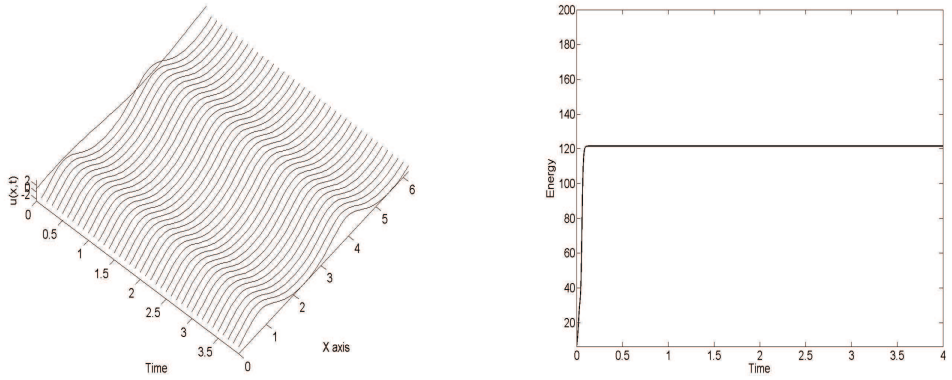

Figure 7: $\beta=30,\varepsilon=0.001,\Delta t=10^{-4}$, the contour of solution (left) and energy (right).

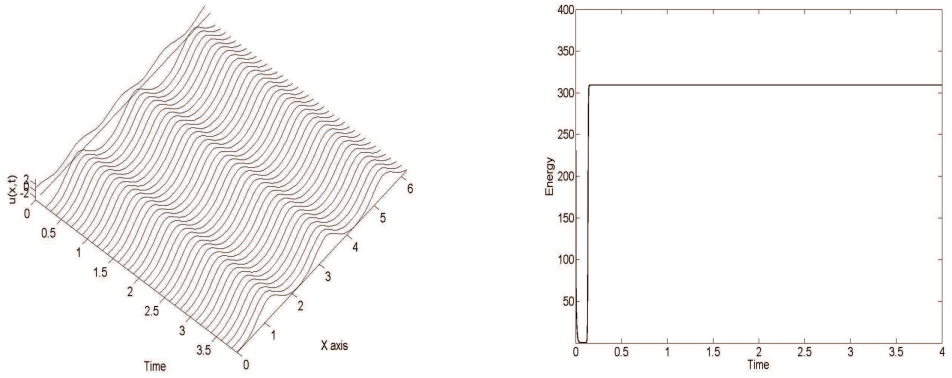

Figure 8: $\beta=60,\varepsilon=0.001,\Delta t=10^{-4}$, the contour of solution (left) and energy (right).

These numerical results indicate that the solution of equation (1.5)-(1.6) preserve the same structure as K-S equation. Richer dynamics can be generated by using even large

β. Finally, we plot in Fig. 9 the front propagation from calculation with $\beta=105$, $u_0(x)=\sin(x)+\cos(x)$, $\varepsilon=0.001$. As expected form the paper ([12], [13]), the front evolves toward an essentially quadrimodal global attractor.

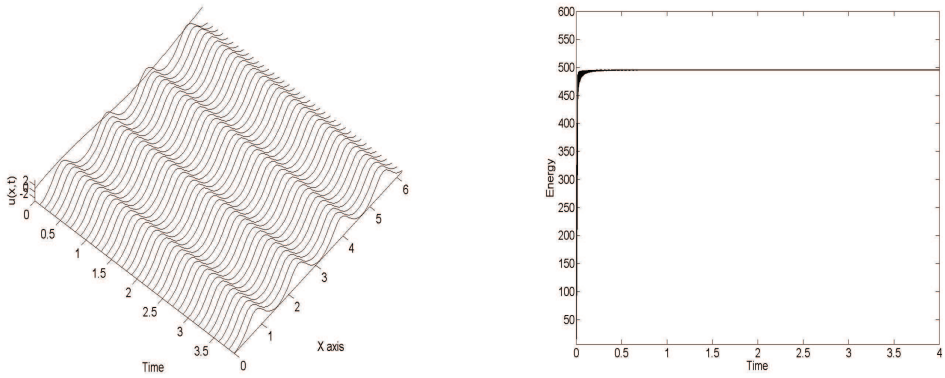

Figure 9: $\beta=105,\varepsilon=0.001,\Delta t=10^{-4}$, the contour of solution (left) and energy (right).

4 Conclusion

In this paper, we constructed and analyzed a schema for the numerical solution of the flame front. The proposed method combines a second order schema for the time discretisation and Fourier spectral method for the spatial discretisation. A discrete energy inequality and error estimates are derived in a particular case. Numerical experiments are carried out to verify the theoretical prediction in one side, and to investigate the behavior of the solution in the other side. Numerical experiments are also provided to indicate that we can choose $\Delta t=O(\varepsilon)$ (at least) such that the flame front equation asymptotically converges to the K-S equation and its solution preserves the same structure as the K-S equation.

Acknowledgments

The work is supported by National Natural Science Foundation of China (No. 11461012) Scientific Research Development Fund of Wenzhou Medical University (No. QTJ11014); Zhejiang Provincial Department of Education Research Project (No. Y201328047), Foundation of Guizhou Science and Technology Department (No. [2013]2128) and "125" Science and Technology Grand Project Sponsored by the Department of Education of Guizhou Province (No. [2012]011).

References

[1] G. Akrivis and Y. S. Smyrlis. Implicit-explicit bdf methods for the kuramoto-sivashinsky equation. *Appl. Numer. Math.*, 51(2):151-169, 2004.

[2] H. Berestycki, S. Kamin, and G. Sivashinsky. Metastability in a flame front evolution equation. *Interfaces and Free Boundaries*, 3(4):361-392, 2001.
[3] J. P. Boyd. *Chebyshev and Fourier spectral methods*. Courier Dover Publications, 2001.
[4] C. M. Brauner, M. Frankel, J. Hulshof, G. I. Sivashinsky, *et al.* Weakly nonlinear asymptotics of the κ-θ model of cellular flames: the qs equation. *Interfaces Free Bound*, 7:131-146, 2005.
[5] C. M. Brauner, J. Hulshof, L. Lorenzi, and G. I. Sivashinsky. A fully nonlinear equation for the flame front in a quasi-steady combustion model. *arXiv preprint arXiv:0910.5322*, 2009.
[6] C. M. Brauner, L. Lorenzi, G. I. Sivashinsky, and C. Xu. On a strongly damped wave equation for the flame front. *Chinese Annals of Mathematics-Series B*, 31(6):819-840, 2010.
[7] C. M. Brauner and A. Lunardi. Instabilities in a two-dimensional combustion model with free boundary. *Archive for rational mechanics and analysis*, 154(2):157-182, 2000.
[8] C. Canuto, M. Y. Hussaini, A. Quarteroni, and T. A. Zang. *Spectral Methods. Scientific Computation*. Springer-Verlag, Berlin, 2006.
[9] B. Costa, W. S. Don, D. Gottlieb, and R. Sendersky. Two-dimensional multi-domain hybrid spectral-weno methods for conservation laws. Technical report, DTIC Document, 2006.
[10] L. Cueto-Felgueroso and J. Peraire. A time-adaptive finite volume method for the cahn-hilliard and kuramoto-sivashinsky equations. *J. Comput. Phys.*, 227(24):9985- 10017, 2008.
[11] A. Ducrot and M. Marion. Two-dimensional travelling wave solutions of a system modelling near equidiffusional flames. *Nonlinear Analysis: Theory, Methods & Applications*, 61(7):1105-1134, 2005.
[12] J. M. Hyman and B. Nicolaenko. The kuramoto-sivashinsky equation: a bridge between pde's and dynamical systems. *Physica D: Nonlinear Phenomena*, 18(1):113-126, 1986.
[13] J. M. Hyman, B. Nicolaenko, and S. Zaleski. Order and complexity in the kuramoto-sivashinsky model of weakly turbulent interfaces. *Physica D: Nonlinear Phenomena*, 23(1):265-292, 1986.
[14] I. G. Kevrekidis, B. Nicolaenko, and J. C. Scovel. Back in the saddle again: a computer assisted study of the kuramoto-sivashinsky equation. *SIAM J. Appl. Math.*, 50(3):760-790, 1990.
[15] A. H. Khater and R. S. Temsah. Numerical solutions of the generalized kuramoto- sivashinsky equation by chebyshev spectral collocation methods. *Computers & Mathematics with Applications*, 56(6):1465-1472, 2008.
[16] L. Lorenzi. A free boundary problem stemmed from combustion theory. part I: Existence, uniqueness and regularity results. *Journal of mathematical analysis and applications*, 274(2):505-535, 2002.
[17] B. J. Matkowsky and G. I. Sivashinsky. An asymptotic derivation of two models in flame theory associated with the constant density approximation. *SIAM J. Appl. Math.*, 37(3):686-699, 1979.
[18] B. Nicolaenko, B. Scheurer, and R. Temam. Some global dynamical properties of the kuramoto-sivashinsky equations: nonlinear stability and attractors. *Physica D: Nonlinear Phenomena*, 16(2):155-183, 1985.
[19] B. Nicolaenko, B. Scheurer, and R. Temam. Some global dynamical properties of a class of pattern formation equations. *Communications in partial differential equations*, 14(2):245-297, 1989.
[20] A. Quarteroni and A. Valli. *Numerical approximation of partial differential equations*, volume 23. Springer and Business Media, 2008.
[21] G. I. Sivashinsky. On flame propagation under conditions of stoichiometry. *SIAM J. Appl. Math.*, 39(1):67-82, 1980.
[22] A. M. Turing. The chemical basis of morphogenesis. *Bulletin of mathematical biology*, 52(1):153-

197, 1990.
[23] D. Xiu, J. Shen, *et al.* An efficient spectral method for acoustic scattering from rough surfaces. *Commun. Comput. Phys.*, 2(1):54-72, 2007.
[24] C. J. Xu and T. Tang. Stability analysis of large time-stepping methods for epitaxial growth models. *SIAM J. Numer. Anal.*, 44(4):1759-1779, 2006.